The Annals of the University Dunarea de Jos of Galati
Fascicle VI – Food Technology (2023), 47(1), 64-78

ORIGINAL RESEARCH PAPER

MAILLARD REACTION PRODUCTS BETWEEN WHEY POWDER AND WATER-SOLUBLE TEMPEH PROTEIN EXTRACT: MEMBRANE-BASED FRACTIONATION

TSANIYAH AYU MAULIASYAM[1], SLAMET BUDIJANTO[1], AZIS BOING SITANGGANG[1*]

[1]*Department of Food Science and Technology, Faculty of Agricultural Engineering and Technology, IPB University, Bogor 16680, Indonesia*

[*]Corresponding author: boing.lipan@apps.ipb.ac.id

Received on 22 July 2022
Revised on 30 March 2023

Abstract

Whey powder, an industrial by-product, has the potential to be transformed into functional ingredients using the Maillard reaction. In this study, this chemical reaction occurred between whey powder and tempeh protein extract, resulting in increased antioxidant activity. This study aimed to isolate the Maillard reaction products (MRP) with the best antioxidant capacity using an ultrafiltration (UF) membrane by considering the fouling phenomenon that occurred on the membrane surface and critical flux for the filtration. MRP exhibited an antioxidant capacity of 0.09 mg ascorbic acid equivalent antioxidant capacity/mL, and the fractionation using a 5 kDa MWCO PES membrane showed the highest antioxidant capacity in terms of free radical reduction and metal chelating mechanisms. During MRP filtration, fouling on the membrane surface was observed, which could be attributed to the cake filtration model. The critical flux value was determined to be 4.23 LMH with a corresponding pressure of 0.75 bar. A long-term filtration below the critical flux showed stable performance, but filtration above the critical flux resulted in significant fouling. The permeate antioxidant IC_{50} value was 4.25 mg/mL. Based on the LC-MS analysis, 1,4-dihydroxy-2-methyl-anthraquinone and ilexin II were found as the potential contributors to the antioxidant activity of MRP. In summary, our study demonstrates that fractionating MRP using UF membrane-based filtration is an effective method for isolating MRP with high antioxidant capacity. Our findings also shed light on the critical flux value and fouling phenomenon during MRP filtration, which are important considerations for scaling up the production process.

Keywords: antioxidant activity, critical flux, fouling phenomenon, Maillard reaction product, whey powder

https://doi.org/10.35219/foodtechnology.2023.1.04

Introduction

Whey, a by-product of the cheese and casein industry, accounts for 85 % of the total milk used (Panesar *et al*., 2012). After clarification and pasteurization, whey can be dried to produce whey powder, which mainly consists of lactose (Prazeres *et al*., 2012). Lactose is a reducing sugar that can undergo a Maillard reaction with amino acids, peptides, or proteins by forming covalent bonds between the aldehyde group of lactose and the amine groups of proteins (Hodge, 1953).

Tempeh is a protein source with a fermentation age of 24-36 hours for consumption (Seumahu *et al*., 2013). Over-fermented tempeh is not suitable for consumption, but it still contains proteins and bioactive peptides that can be used for the Maillard reaction (Nooshkam *et al*., 2019).

The Maillard reaction can occur spontaneously with or without heating (Oliveira *et al*., 2015). However, it can also be carried out in a controlled way. Many studies have investigated Maillard reaction kinetics to produce reaction products with higher functionalities. One of the functional benefits of Maillard reaction products (MRP) is their increased antioxidant activity (Patrignani *et al.*, 2016; Nie *et al*., 2017; Shen *et al.*, 2018). In a previous study by Sitanggang *et al*. (2021a), the controlled Maillard reaction between whey powder and tempeh protein extract resulted in up to 90 % increase in antioxidant activity. This finding highlights the potential for using MRP to enhance the functional properties of food products.

Ultrafiltration (UF) membrane based fractionation can be used to increase the antioxidant capacity of MRP. Compared to other techniques, membrane filtration-based purification is a non-intensive energy method that does not require high temperatures that could potentially cause Maillard reactions to degrade the MRP. However, the UF membrane filtration can be prone to fouling, which can be minimized by considering the membrane size, transmembrane pressure (TMP), or flux conditions during the filtration process. Therefore, the aim of this study was to fractionate MRP between whey powder and tempeh protein extract using a UF membrane by considering the fouling phenomenon during the filtration. Additionally, the study considered the critical flux value required to achieve stable filtration performance while maximizing the antioxidant capacity of the permeate. Overall, this study highlights the potential of UF membrane fractionation as an efficient and effective method for increasing the antioxidant activity of MRP, while also minimizing the risk of fouling and preserving the integrity of the Maillard reaction products.

Materials and methods

Materials

The local tempeh with 4 days of fermentation was from the Koperasi Tempeh Indonesia (Kopti), Bogor, Indonesia. Whey powder was obtained from Fonterra, Indonesia, pure water from OneMed Water, Indonesia, 2,2-diphenyl-1-picrylhydrazyl (DPPH) from HiMedia, India, 2,4,6-tris(2-pyridyl-s-triazine) (TPTZ), Folin-Ciocalteau, methanol, and other chemicals were purchased from

Merck KgaA, Darmstadt, Germany. The UF membrane from Micro Nadir (Germany) is polyethersulfone (PES) with polypropylene backing material measuring 2, 4, 5, 10, and 20 kDa. The membrane has a thickness of 210-250 µm with a wide pH tolerance of 0-14.

Maillard reaction

The Maillard reaction between whey powder and water-soluble tempeh protein extract was performed under the optimized conditions determined in a previous study (Sitanggang *et al.*, 2021a). A 5 % (*w/v*) whey powder was added to the tempeh protein extract, and the mixture was reacted at a pH of 5, an initial temperature of 100 °C, and agitation of 200 rpm for 90 minutes using a hot plate stirrer (CPAK Inter Co. LTD, Thailand). The obtained MRP was separated from the precipitate using filter paper number 43 (Whatman™, China). MRP was characterized in terms of viscosity, antioxidant capacity, total phenolic content, protein content, and °Brix value.

Membrane filtration rig

The filtration rig and the procedure for operating the reactor were according to Sitanggang *et al.* (2021b). The pressure was provided by nitrogen gas, and the amount of pressure was regulated by the proportional pressure regulator which was controlled by the PID controller. The filtration was performed under a dead-end operation. The membrane was cut with a diameter of 4.7 cm and immersed in pure water for 15 minutes before being installed in the membrane reactor. The membrane was then used in pure water filtration at 1 bar for 60 minutes.

Membrane size selection

The fractionation of MRP was accomplished by using membranes with various molecular weight cut-offs (MWCOs) to separate the components according to their molecular weights. The MRP was filtered using membranes with MWCOs of 2, 4, 5, 10, and 20 kDa under a constant transmembrane pressure (TMP) of 1 bar for 120 minutes at a temperature of 26 ± 1 °C with agitation at 300 rpm. The antioxidant capacity, phenolic content, protein content, and °Brix value of the resulting permeate from each membrane were analyzed. The membrane that produced the MRP permeate with the highest antioxidant capacity was selected for critical flux determination.

Fouling phenomenon model determination

In this study, the fouling phenomenon was investigated during the separation of MRP using membrane filtration. To understand the fouling mechanism, four fouling models were employed according to Field *et al.* (1995), such as complete pore blocking, internal pore blocking, particle pore blocking, and cake filtration. The fouling model that occurs on the membrane surface was determined by calculating the mean squared error (MSE) between the model and the actual flux. The model with the smallest MSE was selected as the most appropriate. The optimization was performed using the solver in Microsoft Excel (Microsoft, USA).

Critical flux determination

Filtration was carried out at various constant TMPs (0.5, 0.75, 1, 1.5, 2, 2.5 bar) to observe the effect of increasing TMP on the fouling phenomenon and the characteristics of the MRP permeate, such as antioxidant capacity, phenol content, protein content, and °Brix value. Filtration was performed for 60 minutes at room temperature (26 ± 1 °C) with 300 rpm agitation. The critical flux was determined by TMP and flux stepping, which followed the method of Gesan-Guiziou *et al.* (2002). Each TMP or flux was held constant for 30 minutes before being raised or lowered. There was no membrane switching during the stepping process. The pressure value used during the TMP stepping was the same as in the previous step (0.5, 0.75, 1, 1.5, 2, 2.5 bar). Meanwhile, the flux value used in the stepping flux was based on the value observed during the TMP stepping (2.86, 4.23, 5.57, 8.06, 10.20, 12.25 LMH). The cake resistance profile on the membrane surface as a function of flux and TMP value during stepping along with the membrane resistance was determined using equations 1 and 2, respectively:

$$J = \frac{\Delta P}{\mu s\,(R_m + R_c)} \quad (1)$$

$$J = \frac{\Delta P}{\mu w\, R_m} \quad (2)$$

where *J:* flux (m^3/m^2s); ΔP: transmembrane pressure (Pa); μs: sample viscosity (Pa.s); μa: viscosity of water at 25 °C (0.00089 Pa.s); R_m: membrane resistance (m^{-1}); R_c: cake resistance (m^{-1}).

To determine the membrane resistance, pure water was filtered under the same conditions as the MRP filtration as described by Babel and Takizawa (2010). The critical flux was determined based on the flux value before the deviation point from the linear relationship between the flux and TMP profiles, following the method proposed by Bacchin *et al.* (2006). To evaluate the operating stability of the critical flux, the increase in pressure during filtration was monitored over a longer filtration period. Three different flux values were tested: the critical flux, half the critical flux, and twice the critical flux, as suggested by Kim and DiGiano (2006). The permeate from each flux value was characterized in terms of antioxidant capacity, IC_{50} value, phenol content, protein content, and °Brix value. Moreover, the compounds present in the permeate were identified.

Measurement of viscosity

Viscosity was measured using a Brookfield LVT analog viscometer instrument (AMETEK, USA). Measurements were made using spindle LV-1 number 61 with a speed of 60 rpm so that the multiplier factor was 1. Viscosity measurements were carried out for 60 s (Wood *et al.*, 1963).

Analysis of total phenols content

A 0.2 mL of the sample was mixed with 1.8 mL of Folin-Ciocalteau reagent in a 1:10 ratio (*v/v*). The solution was incubated for 6 minutes, after which 1.8 mL of 6% Na_2CO_3 was added and the solution was incubated again for 90 minutes in a dark place at room temperature (25-30 °C). The absorbance of the resulting solution was measured at a wavelength of 725 nm using UV-Vis spectrophotometry (Thermo Fisher Scientific Inc., USA) (Qiu *et al*., 2010). The total phenols content was expressed as mg/mL gallic acid equivalent (GAE).

Analysis of protein content

A 50 µL volume was mixed with 2.5 mL of Bradford reagent and incubated for 10 minutes at room temperature (25-30 °C). The absorbance of the solution was then measured at a wavelength of 595 nm using a spectrophotometer (Purwanto, 2014). The Bradford reagent relies on the binding of Coomassie Brilliant Blue dye to the basic and aromatic amino acid residues of proteins, such as arginine, histidine, phenylalanine, and leucine (Utami *et al*., 2016). The protein content was expressed in mg/mL bovine serum albumin (BSA) equivalent.

Analysis of antioxidant capacity

The antioxidant capacity of MRP was determined using two methods: the free radical reduction of 2,2-diphenyl-1-picrylhydrazyl (DPPH) and the ferric reducing antioxidant power (FRAP) methods. For the DPPH method, 300 µL of MRP was mixed with 700 µL of distilled water and 3 mL of 80 mM DPPH solution. The solution was then incubated in a dark place at room temperature (25-30 °C) for 30 minutes, after which the absorbance was measured at a wavelength of 515 nm using UV-Vis spectrophotometry (Brand-Williams *et al*., 1995). Meanwhile, for the FRAP method, 150 µL of MRP was mixed with 4.5 mL of FRAP reagent (a mixture of acetate buffer 300 mM pH 3.7, TPTZ 10 mM in 40 mM HCL, and 20 mM $FeCl_3$ in a ratio of 10:1:1). The absorbance was measured at a wavelength of 598 nm using UV-Vis spectrophotometry (Benzie and Strain, 1996). The antioxidant capacity was expressed in mg/mL AEAC (ascorbic acid equivalent antioxidant capacity). The half-maximal inhibitory concentration (IC_{50}) was determined based on the DPPH method. The IC_{50} value was obtained by plotting the MRP concentration against the relative scavenging activity and determining the concentration of MRP that exhibited 50% scavenging activity (Sitanggang et al., 2020).

Measurement of ºBrix

The instrument used to measure °Brix was a portable refractometer (HT214ATC 0-32% Brix). A sample volume of 0.5 mL of MRP was placed on the prism of the refractometer and covered with the plate, ensuring an even distribution and absence of air bubbles. The refractometer prism was then pointed towards a light source, and the scale reading was taken from the other end. The Brix reading was obtained by reading the scale on the refractometer, as described by Schoos *et al*. (2021). .

Compound identification

Compounds in the MRP fraction were identified using liquid chromatography-mass spectroscopy (LC-MS) with an LC Ultimate 3000 Series System and QTOF G2XS

mass spectrophotometer. The mobile phase comprised of two solutions, A and B. The first mobile phase (A) consisted of 0.1% formic acid in water, while the second mobile phase (B) was a mixture of acetonitrile with 0.1% formic acid. The flow rate was adjusted to 0.3 mL/min, and a gradient elution was performed as follows: 5 % B for 1 minute, 40 % B for 7 minutes, 100 % B for 5 minutes, and 5 % B for 3 minutes. After separation by chromatography, the molecular mass was detected by mass spectrophotometry within the mass range of 50-1200 m/z.

Statistical analysis

Data were analyzed using the SPSS Statistics 24 program (IBM, USA) with oneway-ANOVA and Duncan follow-up test. The analysis was carried out with two replications and two repetitions. This study was included in a completely randomized design (CRD).

Results and discussion

Membrane's MWCO selection based on chemical characterization of MRP

Table 1 presents the characteristics of MRP and its fractions. The viscosity of MRP was found to be 3 x 10^{-3} Pa.s. MRP was found to contain several components, including sugar, peptides, phenols, and the Maillard reaction compounds (Laroque *et al*., 2008). The total sugar content in the MRP was 8.75 °Brix. Meanwhile, the protein content was about 4.12 mg BSA/mL. The presence of phenols in MRP was also detected, with a concentration of 0.49 mg GAE/mL. It should be noted that the extraction of tempeh protein may result in the loss of some phenols due to their ability to form hydrogen bonds with water (Froehner *et al.*, 2009).

Table 1. Characteristics of MRP and MRP fractions.

Characteristics	MRP	MRP fraction based membrane's MWCO (kDa)				
		20	10	5	4	2
Total °Brix	8.75±0.25	7.75±0.25^{e}	7.42±0.13^{d}	6.00±0.00^{c}	5.50±0.00^{b}	4.00±0.00^{a}
Protein (mg BSA/mL)	4.12±0.04	0.35±0.01^{e}	0.28±0.01^{d}	0.25±0.00^{c}	0.19±0.01^{b}	0.15±0.01^{a}
Phenol (mg GAE/mL)	0.49±0.01	0.40±0.01^{d}	0.40±0.00^{d}	0.36±0.01^{c}	0.33±0.01^{b}	0.28±0.01^{a}
DPPH (mg AEAC/mL)	0.09±0.01	0.10±0.02^{a}	0.10±0.00^{a}	0.13±0.00^{b}	0.01±0.00^{c}	0.01±0.01^{c}
FRAP (mg AEAC/mL)	0.11±0.03	0.11±0.01^{a}	0.11±0.00^{a}	0.16±0.00^{b}	0.09±0.00^{c}	0.09±0.01^{c}

Numbers followed by different superscript letters in the same row show significant difference with a confidence level of 95 %.

The antioxidant capacity of MRP was found to be influenced by the presence of the Maillard reaction compound, peptides, and phenols, which act through different mechanisms, including electron transfer, metal chelation, and hydrogen transfer (Vhangani and Van Wyk, 2013). MRP exhibited antioxidant activity with an iron

reduction mechanism, with a capacity of 0.11 mg AEAC/mL, while the antioxidant activity with free radical reduction mechanisms was 0.09 mg AEAC/mL.

The permeate from MRP fractionation showed a reduction in °Brix, protein, and phenol content as the membrane size decreased. However, the decrease in protein and phenol did not lead to a decrease in antioxidant capacity, indicating that the presence of the Maillard reaction compound played a significant role in determining antioxidant activity. Melanoidin, which is one of the Maillard reaction compounds, has varying molecular weights ranging from less than 1 kDa to more than 30 kDa, depending on the reacting conditions and the type of reactants (Adams *et al*., 2005). Among the MRP fractions, the permeate filtered with a 5 kDa MWCO membrane showed the highest DPPH and FRAP antioxidant capacity, with values up to 0.13 mg AEAC/mL and 0.16 mg AEAC/mL, respectively. These values were significantly different from the antioxidant capacity of other MRP fractions at the 95% level. The decrease in protein content as the membrane size decreased was due to the various MWs of tempeh proteins, with proteins higher than the membrane size being retained (Barhate *et al*., 2003). Phenol components could form hydrogen bonds with proteins, which could also lead to their retention on the membrane surface (Bartolomé *et al*., 2000). The retention of protein and phenol on the membrane surface as a cake could also cause sugar rejection by the membrane.

Fouling phenomenon during filtration

Fouling is a common problem in membrane filtration and can occur due to various reasons, such as adhesion force between foulant and membrane, interaction among foulants, and blockage of membrane surface. Foulants can be inorganic and organic compounds, colloids, and microorganisms. (Ashfaq *et al*., 2019). In the case of MRP filtration, foulants can be in the form of phenolic components, proteins, lactose, and Maillard reaction by productsc with high MWs.

Table 2 shows the MSE fouling phenomenon for each membrane cut-off. The cake filtration model yielded the smallest MSE for all five membrane sizes. A small MSE suggests that the predicted values were close to the actual values. Hence, the cake filtration model wass the most appropriate to describe the fouling phenomenon on the membrane surface. This implies that the fouling occurring on the membrane surface is likely due to the interaction among MRP components, leading to the formation of a cake layer. Similar cake filtration phenomena have been reported in alginate filtration (You *et al*., 2021) and water treatment (Bu *et al*., 2019). Even though cake filtration allows the sample to flow into the permeate, the flow rate may decrease as the layer of cake on the membrane surface increases during constant pressure filtration.

The permeate flux depends on several factors such as the initial flow rate, membrane area, filtration time, and the fouling constants n and K. The fouling index n is specific to the fouling model that occurs on the membrane surface. On the other hand, the resistance constant K is obtained from model calculations. As the membrane size decreases, the K value of each fouling model shows an increase. This is due to the smaller membrane pore size, which causes more components to be retained on the membrane surface, making it easier for fouling to occur. Consequently, the value of

the resistance constant increases, as observed in previous studies (Hwang *et al*., 2008).

Table 2. Fouling models on five membrane cut-offs.

Model		20-kDa	10-kDa	5-kDa	4-kDa	2-kDa
Complete pore blocking	MSE (10^3)	9.07	7.49	1.40	1.08	0.12
	K	6.10	5.79	7.58	7.44	7.45
Internal pore blocking	MSE	100.79	135.41	17.06	15.07	4.27
	K	0.04	0.05	0.03	0.03	0.06
Particle pore blocking	MSE	69.94	95.46	16.09	13.89	4.11
	K	0.29	0.36	0.33	0.40	1.21
Cake filtration	MSE	29.81	43.92	14.43	11.84	3.83
	K	14.08	19.54	39.10	53.30	482.99

Critical flux during MRP filtration

Figure 1 shows the flux profile during filtration under different pressures. As the initial pressure increased, the obtained flux value also increased. This could be attributed to the increase in the driving force of the sample through the membrane, allowing more permeate volume to pass through per unit time. Filtration at pressures of 0.5 and 0.75 bar demonstrated stability during operation. However, filtration at pressures of 1.0, 1.5, 2.0, and 2.5 bar exhibited a significant decrease in flux over the length of the filtration time. This decrease indicates fouling. The high pressure or flux caused an increase in convective transport (Cancino-Madariaga *et al*., 2012), leading to the formation of a thicker cake layer with increased filtration time.

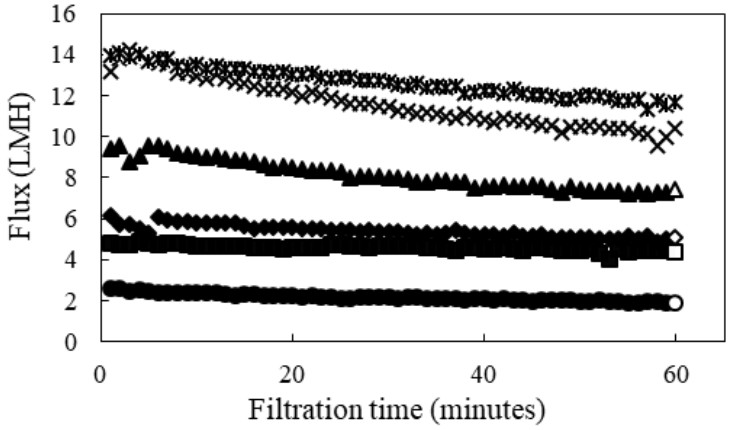

Figure 1. Flux profiles during the filtrations of MRP with (○) 0.5; (□) 0.75; (◇) 1.0; (△) 1.5; (×) 2.0; and (∗) 2.5 bar.

Table 3 presents the characteristics of the permeate. There was no significant difference at the 95% confidence level in the total phenol and protein content of the permeate filtered at pressures ranging from 0.5 to 2.5 bar.

Table 3. Characteristics of MRP permeate under different filtration conditions.

Characteristics	TMP (bar)					
	0.5	**0.75**	**1**	**1.5**	**2**	**2.5**
Total °Brix	4.25 ± 0.559^{a}	4.5 ± 0.000^{b}	5.25 ± 0.250^{bc}	5.00 ± 0.000^{bc}	5.25 ± 0.250^{bc}	5.50 ± 0.000^{c}
Protein (mg BSA/ mL)	0.24 ± 0.004^{a}	0.24 ± 0.009^{a}	0.24 ± 0.005^{a}	0.24 ± 0.010^{a}	0.24 ± 0.008^{a}	0.24 ± 0.010^{a}
Phenol (mg GAE/ mL)	0.33 ± 0.012^{a}	0.34 ± 0.013^{a}	0.34 ± 0.020^{a}	0.33 ± 0.014^{a}	0.036 ± 0.025^{a}	0.036 ± 0.011^{a}
DPPH (mg AEAC/mL)	0.10 ± 0.013^{a}	0.11 ± 0.003^{a}	0.13 ± 0.003^{b}	0.13 ± 0.001^{b}	0.14 ± 0.007^{c}	0.14 ± 0.002^{c}
FRAP (mg AEAC/mL)	0.12 ± 0.025^{a}	0.14 ± 0.007^{a}	0.17 ± 0.005^{bc}	0.16 ± 0.004^{b}	0.17 ± 0.007^{bc}	0.18 ± 0.005^{c}

	Flux (LMH)		
	2.12	**4.23**	**8.46**
Total °Brix	5.06 ± 0.682^{a}	5.69 ± 0.348^{b}	5.06 ± 0.300^{a}
Protein (mg BSA/ mL)	0.17 ± 0.007^{c}	0.13 ± 0.009^{b}	0.10 ± 0.013^{a}
Phenol (mg GAE/ mL)	0.31 ± 0.008^{a}	0.34 ± 0.011^{b}	0.35 ± 0.003^{b}
DPPH (mg AEAC/mL)	0.12 ± 0.008^{b}	0.13 ± 0.003^{c}	0.11 ± 0.001^{a}
FRAP (mg AEAC/mL)	0.19 ± 0.003^{a}	0.21 ± 0.007^{c}	0.20 ± 0.005^{b}
IC_{50} (mg/ mL)	4.53 ± 0.072^{b}	4.25 ± 0.117^{a}	5.25 ± 0.147^{c}

Identification of compounds

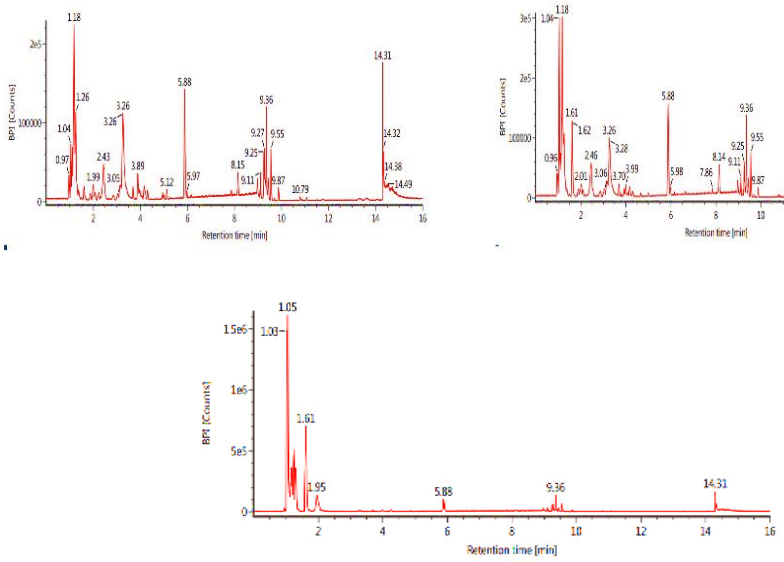

Numbers followed by different superscript letters in the same row show significant difference with a confidence level of 95 %.

However, the total sugar content in °Brix increased as higher pressure was applied. This increase could be due to convective transport, as the higher force applied to the sample caused more components to be transported through the membrane pores (Adrus and Ulbricht, 2012). In addition, the Maillard reaction compounds, especially those with low molecular weight, could also pass through the membrane as the filtration pressure increased. In summary, the antioxidant capacity of the permeate could increase as the filtration pressure increased.

Figure 2 shows the stepping, resistance cake, and flux-TMP relation profile during TMP and flux stepping. Unstable operation was observed during TMP stepping at 1 bar pressure, as indicated by the decreased flux during filtration within a certain period. However, during flux stepping, a significant pressure increase was observed at a flux value of 12.25 LMH with an initial pressure of 2.5 bar. Operation with constant flux was more stable than constant pressure because it could quickly reach a steady state (Bacchin *et al.*, 2006).

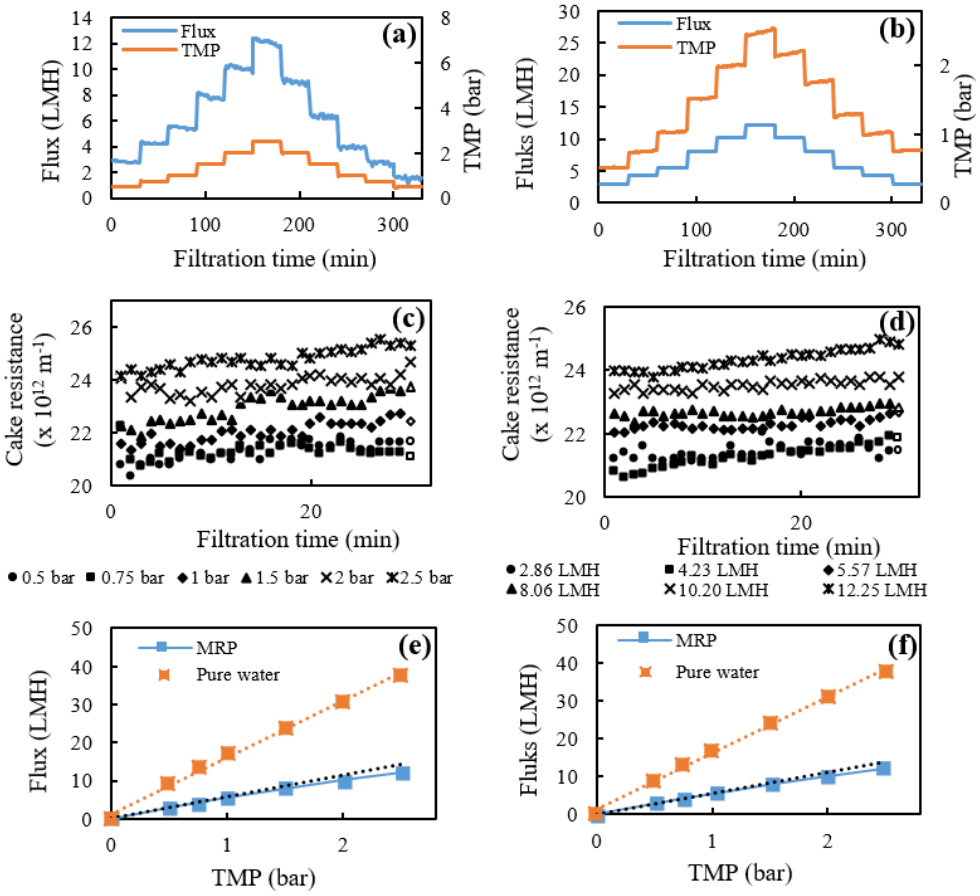

Figure 2. Profile of stepping (a) TMP, (b) flux, resistance cake at constant (c) TMP operation, (d) flux operation, and flux-TMP relation during filtration under constant (e) TMP, (f) flux operation.

Constant pressure operation could lead to faster fouling on the membrane surface due to the applied force, which directly increased the initial operating flux value. In contrast, with constant flux operation, the pressure increased gradually (Field *et al*., 1995; Decloux and Tatoud, 2000). Therefore, operation at a constant flux is preferable for long period of filtration.

The cake resistances for pressures of 0.5 and 0.75 bar and flux values of 2.86 and 4.23 LMH were similar, suggesting that fouling was minimal. However, when the pressure was increased to 1 bar or the flux was increased to 5.57 LMH, cake resistance increased due to greater foulant deposition on the membrane surface (Park *et al*., 2013). The flux-TMP profile showed that a flux of 5.59 LMH at 1 bar deviated from the linear line, indicating significant foulant accumulation on the membrane surface and reduced filtration performance. This effect occurred when the pressure was increased at a constant flux or when the flux was decreased at a constant pressure. The critical flux value, which is the point before the deviation from linearity, was 4.23 LMH at a pressure of 0.75 bar.

Figure 3 shows the pressure profiles during long-term filtrations using flux values of twice the critical flux (8.46 LMH), the critical flux (4.23 LMH), and half the critical flux (2.12 LMH). All three flux values showed a rapid increase in pressure at the beginning of the filtration process. However, the pressure became more constant for filtration using flux values of 2.12 and 4.23 LMH. Filtration using a flux value of 8.46 LMH did not reach a constant pressure and exhibited continuous pressure increase up to 3.68 bar within 16 hours. This was due to the continuous formation of a cake layer on the membrane surface occurring at a higher rate as a result of higher convective transport (Miller *et al*., 2014). Therefore, fouling occurred at a higher rate when using a higher operating flux, above the critical flux.

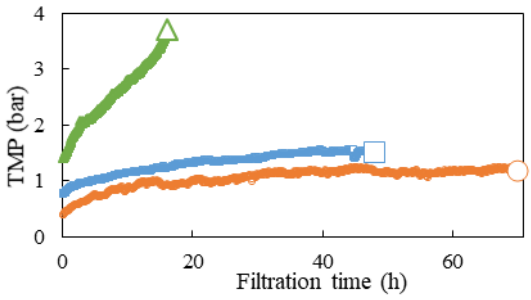

Figure 3. TMP profiles during long-term filtration by (○) half-critical flux (2.12 LMH), (□) critical flux (4.23 LMH), and (△) twice critical flux (8.46 LMH).

Fouling may affect the permeation of different solutes, as shown in Table 3 with the characteristics of the permeate under filtration in relation to the critical flux. A higher flux allows more components, such as phenol, to pass through the membrane, but also leads to faster fouling which retains some components on the membrane surface, such as protein, sugar, and Maillard reaction compounds. The MRP fraction filtered using a flux of 4.23 LMH showed the highest antioxidant capacity. The DPPH

method measured an antioxidant capacity of 0.13 mg AEAC/mL, while the FRAP method measured 0.21 mg AEAC/mL. This value was significantly different at the 95% confidence level compared to the measured antioxidant capacity of the permeate filtered at half-critical flux (2.12 LMH) and twice-critical flux (8.46 LMH). This may be due to the higher pressure during filtration with a flux of 4.23 LMH, which can drive more phenol components and other low molecular weight compounds into the permeate without significant fouling to retain these components on the membrane surface.

The critical flux filtered MRP fraction < 5 kDa exhibited an IC_{50} of 4.25 mg/mL, which was significantly different at the 95% confidence level compared to the permeate obtained from filtration at half and twice critical flux, with IC_{50} values of 4.53 and 5.24 mg/mL, respectively. Although the MRP fraction < 5 kDa from whey powder and water-soluble tempeh protein extract was classified as having a weak antioxidant activity, it was higher than non-fractionated MRP, which exhibited an IC_{50} of 47.82 mg/mL. This suggested that the MRP fraction < 5 kDa was more effective in inhibiting free radicals than non-fractionated MRP. Compared to the MRP from soy concentrate-lactose (47.20 mg/mL) in Oh *et al*. (2013), the antioxidant activity of the MRP fraction in this study was higher. However, it was weaker than the glucose-tyrosine-based Maillard reaction (IC_{50} of 103.09 µg/mL) reported in Ademiluyi *et al*. (2019). The lower antioxidant activity of the MRP fraction could be due to the smaller amount of substrates available, which were bound to peptides and lactose and needed to be degraded first.

The main components found in the MRP of the three permeates included 1,4-dihydroxy-2-methyl-anthraquinone and ilexin II. The compound 1,4-dihydroxy-2-methyl-anthraquinone belongs to the quinone category (Deng *et al*., 2016). Quinones are the phenolic derivative components that have the activity of absorbing radical compounds (Michalik *et al*., 2019). Therefore, 1,4-dihydroxy-2-methyl-anthraquinone can act as an anticancer with a mechanism involving death receptors and apoptosis by mitochondria (Li *et al*., 2016). Likewise, ilexin is included in the phenolic acid group. Phenolic acid is a phenol that is substituted by a carboxyl group. Phenolic acid has a role as antiviral, anticarcinogenic, anti-inflammatory, antibacterial (Sanchez-Maldonado *et al*., 2011), and antioxidant (Kumar and Goel 2019). Ilexin itself has an important role in maintaining the cardiovascular and cerebrovascular systems (Fu *et al*., 2011). In the filtered permeate with half-critical flux value (2.115 LMH), two other main components were identified, namely (-)-Olivil-4',4"-di-O-β-D-glucopyranoside and 5-methoxyfurfural. (-)-Olivil-4',4"-di-O-β-D-glucopyranoside (olivil dg) is a lignan glucoside with antioxidant and anti-inflammatory activity (Yu *et al*., 2022).

Conclusions

Maillard reaction products (MRP) from whey powder and water-soluble tempeh protein extract had an antioxidant capacity of 0.091 ± 0.0127 mg AEAC/mL. MRP fractionation using a PES UF membrane 5 kDa MWCO increased the antioxidant capacity up to 0.1307 ± 0.0019 mg AEAC/mL. Fouling that occurred on the

membrane surface during filtration could be explained by the cake filtration model. Filtration by considering the critical flux value could obtain a stable separation process of MRP. The critical flux value obtained was 4.23 LMH with a corresponding pressure of 0.75 bar. The antioxidant activity of the resulting permeate had an IC_{50} value of 4.25 mg/mL. The permeate contained 1,4-dihydroxy-2-methyl-anthraquinone and ilexin II compounds which could contribute to the antioxidant activity.

References

Adams, A., Borrelli, R.C., Fogliano, V., De Kimpe, N. 2005. Thermal degradation studies of food melanoidins. *Journal of Agricultural and Food Chemistry*, **53**, 4136–4142.

Ademiluyi, A.O., Osalusi, S.E., Oyeleye, S.I., Oboh, G. 2019. Antioxidant properties and inhibitory effects of selected tyrosine-derived Maillard reaction products on α-amylase, α-glucosidase and angiotensin-1 converting enzyme activities. *Biokemistri*, **31**(2), 53-62.

Adrus, N., Ulbricht, M. 2012. Novel hydrogel pore-filled composite membranes with tunable and temperature-responsive size-selectivity. *Journal of Materials Chemistry*, **22**, 3088-3098.

Ashfaq, M.Y., Al-Ghouti, M.A., Qiblawey, H., Rodrigues, D.F., Hu, Y., Zouari, N. 2019. Isolation, identification and biodiversity of antiscalant degrading seawater bacteria using MALDI-TOF-MS and multivariate analysis. *Science of the Total Environment*, **656**, 910-920.

Babel, S., Takizawa, S. 2010. Microfiltration membrane fouling and cake behavior during algal filtration. *Desalination*, **261**(1), 46-51.

Bacchin, P., Aimar, P., Field, R.W. 2006. Critical and sustainable fluxes: Theory, experiments and applications. *Journal of Membrane Science*, **281**, 42-69.

Barhate, R.S., Subramanian, R., Nandini, K.E., Hebbar, H.U. 2003. Processing of honey using polymeric microfiltration and ultrafiltration membranes. *Journal of Food Engineering*, **60**(1), 49-54.

Bartolomé, B., Estrella, I., Hernández, M.T. 2000. Interaction of low molecular weight phenolics with proteins (BSA). *Journal of Food Science*, **65**(4), 617-621.

Benzie, I.F.F., Strain, J.J. 1996. The ferric reducing ability of plasma (FRAP) as a measurement of antioxidant power: the FRAP assay. *Analitical Biochemistry*, **239**, 70-76.

Brand-Williams, W., Cuvelier, M., Berset, C. 1995. Use of a free radical method to evaluate antioxidant activity. *LWT - Food Science and Technology*, **28**(1), 25 – 30.

Bu, F., Gao, B., Yue, Q., Liu C., Wang, W., Shen, X. 2019. The combination of coagulation and adsorption for controlling ultra-filtration membrane fouling in water treatment. *Water*, **11**(90), 1-13.

Cancino-Madariaga, B., Ruby, R., Astudillo Castro, C., Saavedra Torrico, J., Lutz Riquelme, M. 2012. Analysis of the membrane fouling mechanisms involved in clarified grape juice ultrafiltration using statistical tools. *Industrial & Engineering Chemistry Research*, **51**(10), 4017-4024.

Decloux, M., Tatoud, L. 2000. Importance of the control mode in ultrafiltration: case of raw cane sugar remelt. *Journal of Food Engineering*, **44**(2), 119-126.

Deng, L., Shi, A., Liu, H., Meruva, N., Liu, L., Hu, H., Yang, Y., Huang, C., Li, P., Wang, Q. 2016. Identification of Chemical ingredients of peanut stems and leaves extracts using UPLC-QTOF-MS coupled with novel informatics UNIFI platform. *Journal of Mass Spectrometry*, **51**(12), 1157-1167.

Field, R.W., Wu, D., Howell, J.A., Gupta, B.B. 1995. Critical flux concept for microfiltration fouling. *Journal of Membrane Science*, **100**(3), 259-272.

Froehner, S., Martins, R.F., Furukawa, W., Errera, M.R. 2009. Water remediation by adsorption of phenol onto hydrophobic modified clay. *Water Air Soil Pollut*, **199**, 107–113.

Fu, X.C., Xu, Z., Xu, J.Z. 2011. Effects of Mao-Dong-Qing R4 on cardiac function and hemodynamics in anesthetized dogs. *Chinese Journal of Integrative Medicine on Cardio/Cerebrovascular Disease*, **9**(12), 1471-1473.

Gesan-Guiziou, G., Wakeman, R.J., Daufin, G. 2002. Stability of latex crossflow filtration: cake properties and critical conditions of deposition. *Chemical engineering Journal*, **85**, 27-34.

Hodge, J.E. 1953. Chemistry of browning reactions in model systems. *Journal of Agricultural and Food Chemistry*, **1**(15), 928–943.

Hwang, K., Liao, C., Tung, K. 2008. Effect of membrane pore size on the particle fouling in membrane filtration. *Desalination*, **234**, 16-23.

Kim, J., DiGiano, F.A. 2006. Defining critical flux in submerged membranes: Influence of length-distributed flux. *Journal of Membrane Science*, **280**(1), 752-761.

Kumar, N., Goel, N. 2019. Phenolic acids: natural versatile molecules with promising therapeutic applications. *Biotechnology Reports*, **24**, 1-10.

Laroque, D., Inisan, C., Berger, C., Vouland, E., Dufossé, L., Guérard, F. 2008. Kinetic study on the Maillard reaction: Consideration of sugar reactivity. *Food Chemistry*, **111**, 1032-1042.

Li, F., Liu, W., Yamaki, K., Liu, Y., Fang, Y., Li, Z., Chen, M., Wang, C. 2016. Angiotensin I-converting enzyme inhibitory effect of Chinese soypaste along fermentation and ripening: Contribution of early soybean protein borne peptides and late Maillard reaction products. *International Journal of Food Properties*, **19**(12), 2805–2816.

Michalik, M., Poliak, P., Lukes V., Klein, E. 2019. From phenols to quinones: Thermodynamics of radical scavenging activity of para-substituted phenols. *Phytochemistry*, **166**, 112077.

Miller, D.J., Kasemset, S., Paul, D.R., Freeman, B.D. 2014. Comparison of membrane fouling at constant flux and constant transmembrane pressure conditions. *Journal of Membrane Science*, **454**, 505-515.

Nie, X., Xu, D., Zhao, L., Meng. X. 2017. Antioxidant activities of chicken bone peptide fractions and their Maillard reaction products: Effects of different molecular weight distributions. *International Journal of Food Properties*, **20**(1), 457–466.

Nooshkam, M., Varidi, M., Bashash, M. 2019. The Maillard reaction products as food-born antioxidant and antibrowning agents in model and real food systems. *Food Chemistry*. **275**, 644-660.

Oh, N.S., Lee, J.Y., Joung, J.Y., Lee, K.B., Kim, Y., Lee, K.W., Kim, S.H. 2013. The dual effects of Maillard reaction and enzymatic hydrolysis on the antioxidant activity of milk proteins. *Journal of Dairy Science*, **96**(8), 4899-4911.

Oliveira, F.C., Coimbra, J.S.R, Oliveira, E.B., Zuninga, A.D.G, Rojas, E.E.G. 2015. Food protein-polysaccharide conjugates obtained via the Maillard reaction: A Review. *Critical Reviews in Food Science and Nutrition*, **56**(7), 1108-1125.

Panesar, P.S., Kennedy, J.F. 2012. Biotechnological approaches for the value addition of whey. *Journal Critical Reviews in Biotechnology*. **32**(4), 327-348.

Park, M., Lee, J., Boo, C., Hong, S., Snyder, S.A., Kim, J.H. 2013. Modelling of colloidal fouling in forward osmosis membrane: effects of reverse draw solution permeation. *Desalination*, **314**, 115-123.

Patrignani, M., Rinaildi, G.J., Lupano, C.E. 2016. In vivo effects of Maillard reaction products derived from biscuits. *Food Chemistry*, **196**, 204-210.

Prazeres, A.R., Carvalho, F., Rivas, J. 2012. Cheese whey management: a review. *Journal of Environmental Management*, **110**, 48–68.

Purwanto, M.G.M. 2014. Perbandingan analisa kadar protein terlarut dengan berbagai metode spektroskopi uv-visible. *Jurnal Ilmiah Sains dan Teknologi*, **7**(2), 64-71.

Qiu, Y., Liu, Q., Beta, T. 2010. Antioxidant properties of commercial wild rice and analysis of soluble and insoluble phenolic acids. *Food Chemistry*, **121**(1), 140-147.

Sanchez-Maldonado, A.F., Schieber A, Ganzle, M.G. 2011. Structure-function relationships of the antibacterial activity of phenolic acids and their metabolism by lactic acid bacteria. *Journal of Applied Microbiology*, **111**(5), 1176-1184.

Schoos, A., De Spiegelaere, W., Cools, A., Pardon, B., Van Audenhove, E., Bernaerdt, E., Janssens, G.P.J., Maes, D. 2021. Evaluation of the agreement between Brix refractometry and serum immunoglobulin concentration in neonatal piglets. *Animal*, **15**(1), 100041-8.

Seumahu, C.A., Suwanto, A,. Rusmana, I., Solihin, D.D. 2013 Bacterial and fungal communities in tempe as reveal by amplifified ribosomal intergenic sequence analysis. *HAYATI Journal of Bioscience*, **20**(2), 65-71.

Shen, Y., Tebben, L., Chen, G., Li, Y. 2018. Effect of amino acids on Maillard reaction product formation and total antioxidant capacity in white pan bread. International *Journal of Food Science and Technology*, **54**(4), 1-9.

Sitanggang, A.B., Lesmana, M., Budijanto, S. 2020. Membrane-based preparative methods and bioactivities mapping of tempe-based peptides. *Food Chemistry*, **329**(1), 127193.

Sitanggang, A.B., Firdausi, N.Z., Budijanto, S. 2021a. Antioxidant activity of a mixture of water-soluble tempeh extract with whey powder that has undergone a Maillard reaction. *Future of Food: Journal on Food, Agriculture and Society*, **9**(5), 1-12.

Sitanggang, A.B., Sumitra, J., Budijanto, S. 2021b. Continuous production of tempe-based bioactive peptides using an automated enzymatic membrane reactor. *Innovative Food Science & Emerging Technologies*, **68**, 102639-102648.

Utami, P., Lestari, S., Lestari, S.D. 2016. Pengaruh metode pemasakan terhadap komposisi kimia dan asam amino ikan seluang (Rasbora argyrotaenia). *Jurnal Teknologi Hasil Perikanan*, **5**(1), 73-84.

Vhangani, L.N., Van Wyk, J. 2013. Antioxidant activity of Maillard reaction products (MRPs) derived from fuctose-lysine and ribose-lysine model systems. *Food Chemistry*, **137**, 92-98.

Wood, J.H., Catacalos, G., Lieberman, S.V. 1963. Adaptation of commercial viscometers for special applications in pharmaceutical rheology I: the Brookfield viscometer. *Journal of Pharmaceutical Sciences*, **52**(3), 296-298.

You, X., Zhang, J., Shen, L., Li, R., Xu, Y., Zhang, M., Hong, H., Yang, L., Ma, Y., Lin, H. 2021. Thermodynamic mechanisms of membrane fouling during filtration of alginate solution in coagulation-ultrafiltration (UF) process in presence of different ionic strength and iron(III) ion concentration. *Journal of Membrane Science*, **635**, 1-8.

Yu, M., Aoki, D., Akita, T., Fujiyasu, S., Takada, S., Matsushita, Y., Yoshida, M., Fukushima, K. 2022. Distribution of lignans and lignan mono/diglucosides within *Ginkgo biloba* L. stem. *Phytochemistry*, **196**, 113102.